Silicon (2022) 14:8993–9007
https://doi.org/10.1007/s12633-022-01679-7

ORIGINAL PAPER

Experimental and Theoretical Yield Strength of Silicon Carbide and Hexagonal Boron Nitride Reinforced Mg-Zn Nanocomposites Produced by the Combined Effects of Ultrasonication and Squeeze Casting

K. Parthiban[1] · Poovazhagan Lakshmanan[2] · A. Gnanavelbabu[3]

Received: 3 November 2021 / Accepted: 10 January 2022 / Published online: 20 January 2022

Abstract
In this work, an attempt has been made to fabricate novel hybrid nanocomposites from Mg-Zn-Yttrium (traceable) alloy with 1.0 wt. percent nano-SiC_P (fixed) and 0.5, 1.0, and 1.5 wt. percent nano-hBN_P as reinforcing particles. The combined effect of stir-ultrasonication and squeeze casting was applied to mix the nanoparticles in the Mg matrix. The nanocomposite samples were heat-treated at T5 condition. Optical microscopy evaluates the refined grains. SEM pictures represent the uniform nanoparticle dispersion in the Mg matrix. As compared with base alloy, higher dislocation density is observed in the nanocomposite samples which were confirmed by the TEM images. XRD validates the occurrence of SiC and BN phases in the hybrid nanocomposites. The combination of 1.0 wt% SiC_P and 1.5 wt% hBN_P reinforced hybrid nanocomposite show 31% more microhardness and 42% more tensile strength than the base alloy. Various strengthening models employed to assess the influence of nanoparticles on yield strength, which were then, compared to the experimental yield strength values. Experimental and theoretical yield strength values were found to be in closer agreement.

Keywords Ultrasonication · Squeeze casting · Mg-Zn alloy · SiC · Hybrid nanocomposites · SEM · TEM · Yield strength · Strengthening models

1 Introduction

Being a lightweight structural metal, Magnesium (Mg) alloys are the best alternative material for replacing stainless steel, titanium and aluminum [1, 2] in the automobile sector. Magnesium has the exceptional structural properties to be used in road transport, aircraft, and defense factories. It is owing to its low density, good specific strength, and better resistance to wear [3]. Magnesium matrix composites have a few distinct benefits like better castability, excellent electromagnetic shielding, the easiest machining of all structural metals, a high damping capacity, and a lower energy requirement for production. Magnesium has several limitations, like low ductility and elastic modulus, poor mechanical properties at elevated temperature, lower resistance to creep, and a high rate of corrosion. Magnesium nanocomposites have been developed to overcome these limitations by incorporating reinforcements in the nanoscale [1, 4, 5]. The addition of alloying elements in Mg tends to improve their mechanical properties and corrosion resistance [6]. Alloying elements like zinc (Zn), zirconium (Zr), calcium (Ca), and other unique ore components greatly enhance the physical and corrosion resistance properties of Mg [7].When added to Mg alloys, rare earth elements (RE) tend to increase the corrosion resistance and high-temperature resistance properties. Because of their excellent mechanical characteristics and biodegradability, Mg-RE alloys are gaining significant attention in biomedical applications as potential implant materials [6, 8]. At together room and elevated temperatures,

✉ Poovazhagan Lakshmanan
poovazhaganl@ssn.edu.in

[1] Department of Mechanical Engineering, A K T Memorial College of Engineering and Technology, Kallakurichi, Tamilnadu, India

[2] Departments of Mechanical Engineering, Sri Sivasubramaniya Nadar College of Engineering, Chennai, Tamilnadu, India

[3] Departments of Industrial Engineering, Anna University, Chennai, Tamilnadu, India

Mg-Zn-RE alloys have shown improved strength and corrosion resistance properties [9]. The main alloying components in Mg-Zn are zinc (4 wt. percent) and rare earth metals (traceable Amount). As reported in several published research articles, metal matrix nanocomposites (MMNCs) made of Mg has been typically strengthened by materials such as silicon carbide (SiC_P) and aluminum oxide (Al_2O_3). Magnesium -MMNCs provided superior hardness, high resistance to wear, and better tensile strength characteristics than their Mg-based alloys [10, 11]. The strength and tribological characteristics of the composites were determined by several parameters, including the reinforcement content, the size of the particle, the phase of the reinforcement, and the fabricating method used [12]. However, the MMNCs reinforcement with micro-sized ceramic particles may significantly reduce the ductility of the alloy matrix. The MMNCs reinforced with particulates of nano-size to enhance the properties of the matrix by retaining their ductility and augmenting the creep resistance because of its substantial surface area to volume ratio (1000 times greater) as compared with the microparticles [13–15]. The addition of very low volume fractions nano-ceramic particles in Mg matrix drastically improves the mechanical characteristics like compressive yield strength [16]. The excellent characteristics of SiC particles such as high hardness, low thermal expansion coefficient, good corrosion resistance, high thermal stability, high melting point, and low density make them an attractive reinforcement material for lightweight alloy matrix-like Mg [13, 17]. The SiC nanoparticles restrict the movement of the dislocations when applying external loads to the matrix. Numerous experiments have demonstrated that incorporating SiC nanoparticles into a metal matrix increases the contact surface friction. Adding a suitable solid lubricant to the SiC reinforced metal matrix composite (MMC) materials do lower the coefficient of friction and enhance their wear behavior during dry sliding to protect the machine components from excessive friction and wear. By incorporating two distinct nanoparticles into a metal matrix, hybrid nanocomposites are manufactured. The researchers have proposed SiC_p as a primary reinforcement and solid lubricants like hBN_P and graphite as a secondary reinforcement in the matrix material to examine the wear characteristics of MMCs [12]. This addition improves the wear characteristics of nanocomposites of Mg/SiC while lowering the coefficient of friction. Hexagonal boron nitride (hBN_P) is an excellent reinforcing material for MMCs which makes the composites harder and self-lubricating [18]. Earlier research has indicated that incorporating graphite into MMNCs has lowered the composites wear rate. However, as the operating temperature is increased, it's lubricating capacity decreases. The formation of brittle interfacial phases, which reduces the composites strength, is a major limitation of graphite reinforced MMNCs [19]. Graphite materials react with most of the metal matrix alloys during processing, resulting in the development of brittle interfacial phases, which reduces the strength of the composite. Typically, magnesium alloys are very soft and offer lesser resistance to wear. In hybrid nanocomposites, double phases of two different reinforcements contribute significantly to particle strengthening. The manufacturing methods such as mechanical alloying, stir casting, squeeze casting, powder metallurgy, spray deposition and friction stir processing were investigated. Hard nano-reinforcement particle dispersion in molten magnesium matrix is time consuming and expensive. Through liquid metallurgical procedures like compo casting and stir casting, dispersing nano-reinforcement particles is difficult because of the nanoparticles' high surface area to volume ratio and low matrix wettability. Various liquid state metallurgical procedures have been modified by researchers and the ultrasonic-assisted stir casting process has been developed. The dispersion and scattering of ceramic nano elements determine the quality of MMNCs produced [20]. As compared with conventional stirring techniques, the ultrasonic-assisted casting approach exhibited superior distribution and spreading of nanoparticles in metal matrix with improved material characteristics [10]. Additionally, nanocomposites with a refined and uniform grain structure demonstrate superior mechanical and tribological properties. To alter the microstructure of Mg-based composites, several sophisticated material processing methods have recently been developed. Among them, the ultrasonic-assisted casting technique is receiving considerable attention for its ability to refine the grain structure and better particle dispersion [13]. The scattering of ceramic nanoparticulates in molten liquid is highly subjected to variety of factors, including sonication time, ultrasonic pressure, nanoparticle weight%, processing temperature, and ultrasonic intensity [12]. During sonication in molten material is the generation of high-intensity acoustic streaming and transient cavitation. Transient cavitation and acoustic streaming assist in dispersing the clustered nanoparticles, refining grain size, removing porosity, and establishing a homogenous structure. Transient micro hot spot with extremely high pressure and temperature are created by ultrasonic cavitation in the molten melt. Nano clusters are efficiently broken up by these micro hot spots. Additionally, it enhances the wettability of reinforced particles in the molten melt. Simultaneously, acoustic streaming accelerates the mobility and uniform dispersion of nanoparticles in molten melt [19, 21, 22]. Squeeze casting involves forcing and pressurizing the molten material inside the permanent mold to achieve complete densification. Additionally, because of the fast heat transfer rate of the melt, the matrix alloy grain refinement was also observed. It is used to avoid casting imperfections and improve mechanical characteristics. The performance of composites made by squeeze casting is affected by the reinforcing particles, the die

temperature, and squeezing pressure. Squeezing pressure is the most influential factor in improving yield and ultimate tensile strength [23, 24].

Numerous literatures have proposed that the ultrasonic-assisted casting technique has helped in improving the mechanical characteristics of materials. Apratim Khandelwal et al. [25] proposed an ultrasound-stir casting technique to fabricate AZ31/Al_2O_3 Mg alloy nanocomposites. The impact of ultrasonication (UST) and alumina nanoparticles in solidification were investigated under two dissimilar conditions (isothermal-UST and air cooled-UST). Better tensile characteristics, less porosity, and increased ductility are associated with air-cooled UST processing conditions. Isothermal–UST process produced 17% higher hardness, higher porosity, and reduced ductility. Hajo Dieringa et al. [26] manufacturedAM60-based MMNCs using an stir-ultrasonication permanent mold casting technique. The inclusion of AlN nanoparticles improves the YS by 103% and UTS by 115%. Farzan Barati et al. [27] used an ultrasound-assisted casting technique to develop an AM60-SiO_2 nanocomposite. The use of SiO_2 nanoparticles reduces the size of the Mg alloy crystals, increasing the sample's compressive strength and hardness (34.8 HV to 51.5 HV). With the use of an ultrasonically assisted casting method, Abdollah Saboori et al. [28] effectively produced Mg nanocomposites with Elektron21 as the matrix and reinforcement as AlN nanoparticles. The inclusion of AlN nanoparticles reduces grain size while increasing the hardness in 12.7%. Qiang et al. [29] utilized an ultrasonically assisted casting method to manufacture Al-SiC nanocomposites. The SiC nanoparticles were evenly dispersed throughout the matrix and minimal dendritic size is minimal. Due to the strengthening impact of SiC nanoparticles, the strength of Al-SiC nanocomposites increased 217.1%. Harichandran et al. [19] used an ultrasonically assisted casting process to synthesize hybrid Al-B_4C-hBN nanocomposites. The tensile strength of Al-6wt% B_4C nanocomposites was enhanced 40% Also, the elongation of Al-2wt% B_4C-2wt% hBN hybrid nanocomposites was significantly better than other combinations. Afsaneh et al. [30] used an ultrasonically aided casting process to create hybrid Al-Al_2O_3-TiB_2 nanocomposites. The grain refining and Orowan strengthening mechanisms enhanced the strength of hybrid nanocomposites 271%. Shulin et al. [31] used an ultrasonically assisted casting process to fabricate Al-SiC nanocomposites. Dry ball milling was used to treat SiC nanoparticles then dispersed in molten metal. The ultrasonication method decreased the grain size, increase strength 25% and improves the uniformity in the dispersion of SiC nanoparticles. J. Li et al. [13] studied the ultrasonication method, which is commonly employed to achieve homogenous dispersal of micro/nano-sized components in composites made of aluminum alloys. Optimize the matrix and ceramic reinforcements' wettability while retaining a low porosity. To make A356-20 wt% SiC composites, Soundararajan et al. [23] employed mechanical stirring and an ultrasonic-assisted squeeze casting method. When compared to mechanically stirred composites, the outcomes demonstrate that composites treated ultrasonically have superior mechanical and physical characteristics, 12.7% increases strength and 20% increases hardness. Junxiang Zhou et al. [32] synthesized an AM60- alumina (Al_2O_3) fibre and nano-sized Al_2O_3 Magnesium nanocomposite material and investigated the influence of Al_2O_3 hybrid particle. They observe a significant improvement in tensile strength (26.31%) and microstructure confirm the grain refinement. M. Gupta et al. [1] stated that enhancement in strength and ductility in hybrid nanocomposites made of Mg is because of the presence of ceramic reinforcements in nano-size. E. Suneesh et al. [33] investigated Comprehensive studies of magnesium based hybrid composite. Various types of reinforcement effects in mechanical properties and metallurgical characteristics were studied.

Compared to nanocomposites, it has been noted in the literature that hybrid nanocomposites are a superior choice. However, previous research works employed micro level ceramic particles as secondary reinforcements or the ultrasonic assisted technique was used to produce different combinations of reinforcement. In this work, attempts were made to fabricate the hybrid nanocomposites with different hBN_p (0%, 0.5%, 1%, 1.5%) content and fixed content (except base alloy casting) of 1% SiC_p nanoparticles reinforced with Mg-Zn alloy using ultrasonic vibration-assisted squeeze casting technique and further subjected to T5 heat treatment condition. Lightweight materials are required in most of the automobile and aircraft sectors. Hybrid nanocomposites are considered a category of lightweight materials. While mixing the reinforcing nanoparticles in the metal melt, they tended to agglomerate. This is the major issue in the fabrication of hybrid nanocomposites. This research combines the effect of ultrasonication and squeeze casting for fabricating hybrid nanocomposites. Hybrid nanocomposites have the potential to replace aluminum, steel, and titanium in some applications. Sonication assisted casting followed by squeeze casting is a relatively new approach for producing hybrid nanocomposites. The incorporation of two nano-sized reinforcements such as hBN and SiC in Mg-Zn alloy is newly attempted. The calculation of yield strength from various strengthening models for hybrid nanocomposites was not attempted previously. The mechanical characteristics and microstructure of the MMNCs were investigated and compared to the matrix alloy. Hybrid nanocomposites strengthening mechanisms were discussed systematically.

Table 1 Properties of Mg-Zn, SiC_p, and hBN_P

Material	Density (gcm^{-3})	Melting point (°C)	Elastic modulus (GPa)	Co-efficient of thermal expansion (10^{-6} m m^{-1} C^{-1})	Thermal conductivity (Wm^{-1} K^{-1})
Mg-Zn	1.85	638	46	28.4	96
SiC_P	3.20	2730	410	4.6	120
hBN_P	2.29	2527	710	4.563	27

Table 2 Chemical composition of Mg-Zn

Mg-Zn	Zn%	RE%	Zr%	Mg
	4.1	Traceable	0.5	Balance

2 Experimentations

2.1 Materials Used

The matrix alloy was a commercially available Mg-Zn alloy with traceable Yttrium obtained from Nextgen Steel & Alloys (P) ltd., Mumbai, India. Nanoparticles of Silicon carbide (SiC_P-50nm) were acquired from the US Research Nanomaterials laboratory, USA, was employed as primary reinforcement. Secondary reinforcement was chosen as Nanosized Hexagonal Boron Nitride (hBN_P-60nm) procured from Intelligent Materials Pvt Ltd, India. Tables 1 and 2 describe the characteristics and chemical constitutions of the matrix as well as reinforcement materials.

2.2 Experimental Setup

The ultrasonication-assisted squeeze casting system utilized to make the MMNC samples is indicated in Fig. 1. The arrangement includes a resistance heating furnace, an ultrasonic unit, thermocouples, preheating equipment, and an argon supply unit. The ultrasonic unit uses 2.5 kW power, 20 kHz frequency and a 20mm diameter titanium horn. Leak-proof bottom pouring mechanisms with multilayered insulation was provided in the furnace. The bottom pouring arrangement facilitates the injection of molten material into the squeeze casting layout die through an electrically heated route. A squeeze casting system with a hydraulic power press of 50 tons is utilized to increase the densification and reduce the porosity.

2.2.1 Experimental Procedure

The furnace was preheated to 800 degrees Celsius, and then Mg-Zn alloy weighing 1 kg was melted in it. A thermocouple is installed within the furnace to measure the temperature of the liquid melt. Melting was done under the protection of SF6 (10%) and Argon (90%). No additional undesirable

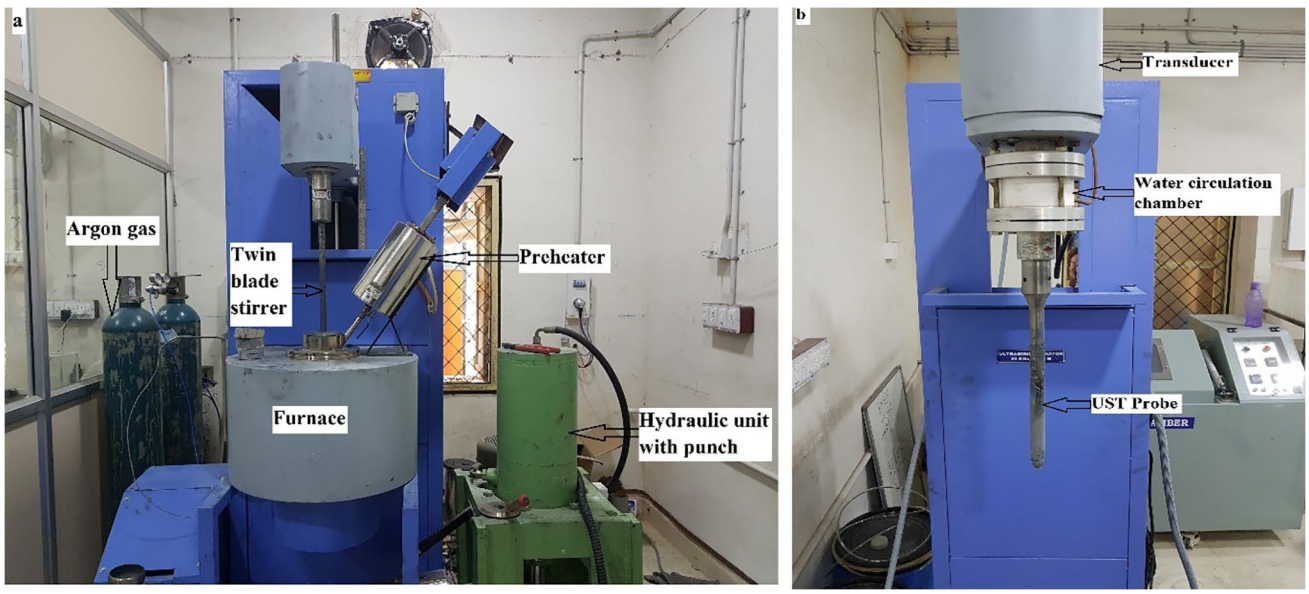

Fig. 1 (**a**) Magnesium Squeeze casting setup and (**b**) Titanium Ultrasonication probe

components formed during the fabrication of metal matrix nanocomposites. The formation of undesirable components during the casting process was effectively prevented by SF_6 (10%) and Argon (90%) gas environment.SF_6 has been found to be an excellent oxidation inhibitor. It forms MgF_2 layer on the liquid metal surface. MgF_2 layer further inhibits the formation of any undesirable components. Figure 2 shows the process of the novel technique used in the experimentations. To create a homogenous alloy mixture, the molten metal was stirred at 500 rpm for 2 min. The pre-heated SiC_p and hBN_P nanoparticles (400 °C for 30 min) were gradually included with the molten material. To primarily mix the nanoparticles, mechanical stirring was continued for another five minutes. It reduces the time required for sonication. After spreading the melt using mechanical stirring, the stirrer was withdrawn from the melt. The sonication probe was submerged in liquid melt to 30mm depth, and the ultrasonic wave generator was activated. Ultrasonic processing was carried out for 10 min for all the experiments. The ultrasonic generator with titanium horn was helps in generating the ultrasonic cavitation effect at 20 kHz frequency. When the strength of ultrasonic waves exceeding the Mg binding energy of the liquid melt during ultrasonic processing, the liquid bonds are broken, and cavitation bubbles develop within the liquid melt. The surrounding particles scattered randomly in all directions after the implosion of the cavitation bubbles during the change in the pressure cycle. After efficient ultrasonic processing, the agglomeration tendencies of nanoparticles were reduced to a significant amount.

Since the hBNp tends to float during fabrication due to its low density, the authors made use of a special type of casting called sonication-assisted squeeze casting system. The high-intensity cyclic ultrasonic waves in magnesium melt create nonlinear sonication effects, like transient cavitation and acoustical streaming. The acoustic streaming effect generates a tumble motion inside the crucible, thus hBNp present in the surface of the molten magnesium is pulled into the melt during the ultrasonication process. Simultaneously, the nonlinear effects produce thousands of transient cavitation bubbles. These cavitation bubbles expand and compress during the cyclic process. When the pressure of the bubble is above the threshold level, they are not able to hold the high pressure. Hence, the bubbles will suddenly implode. The sudden implosions of cavitation bubbles randomly scatter the nanoparticles in the liquid melt. This ensures the uniform dispersion of nanoparticles in the liquid melt. The wettability of nanoparticles and Mg matrix were improved in two stages. Before adding the nanoparticles to liquid metal, they were preheated. Preheating of nanoparticles improves the wettability (bonding). During the sonication-assisted casting process, ultrasonic vibration also improves the wettability between the reinforcing nanoparticles and the metal matrix [17, 34, 35].

By adding nanoparticles of SiC and hBN, the molten liquid material viscosity increased slightly, obstructing the liquid metal's smooth flow into the preheated steel die. Therefore, reheating was done to 800 °C after an efficient sonication process. At last, the liquefied metal was put inside a split type of squeeze die that was compressed for 1 min at 125 MPa and preheated to 400 °C.The diameter and height of the casting ingots obtained, as illustrated in Fig. 3, are 50 mm and 260 mm, respectively. 1HNC (Mg-98.5%, hBN-0.5%, SiC-1%), 2HNC (Mg-98%, hBN-1%, SiC-1%), and 3HNC (Mg-97.5%, hBN-1.5%, SiC-1%) are the names of the nanocomposites that were created (except base alloy casting). The composite materials were thermally treated at T5 in an argon-gas-protected atmosphere in a muffle furnace. Heat-treatment was done for 2 h at 330 °C, and then cooled in air. After that, 16 h of aging at 180 °C was followed by air chilling.

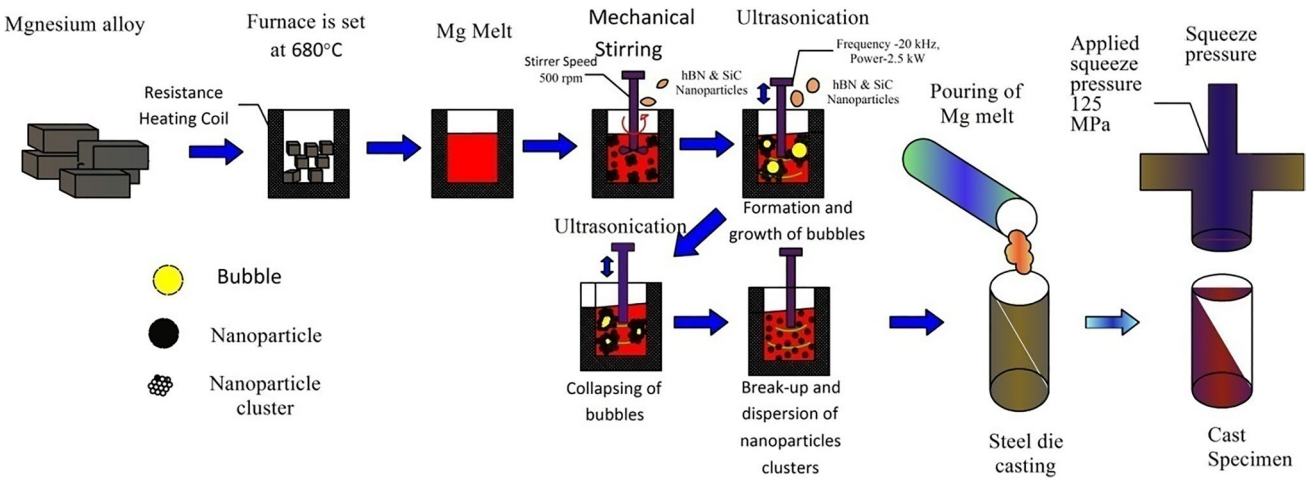

Fig. 2 Sketch of the novel fabrication process

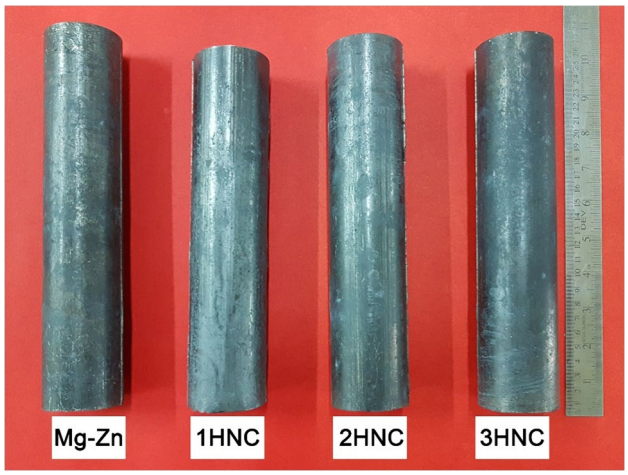

Fig. 3 Cast nanocomposite specimens

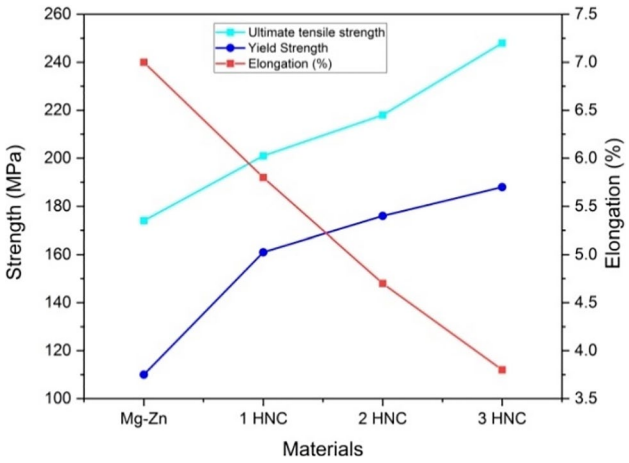

Fig. 5 Strength properties of monolithic alloy and MMNCs

3 Results and Discussion

3.1 Tensile Studies

The standard ASTM E8 samples were prepared for tensile testing. Surface defects were removed by polishing the specimens with abrasive sheets made up of silicon carbide with 300 to 800 grit size. Universal tensile testing (UTM) equipment with10 kN load cell and 0.1 mm/min crosshead speed was employed for tensile studies. The engineering stress-strain curve for monolithic alloy and hybrid MMNCs is displayed in Fig. 4. The variation in UTS, YS and elongation (%) values of the monolithic Mg and hybrid nanocomposites are presented in Fig. 5. The nanocomposites have higher values of UTS and YS than the basic Mg alloy. The augment of UTS and YS of nanocomposites are attributed to the strengthening effect of Hall-Petch, thermal mismatch (high dislocation density) and Orowan bowing produced by the nanoparticles. The load sharing effect has a negligible impact on the mechanism of nanoparticle reinforced composites [36]. In comparison to the base alloy, the variance in CTE and tensile modulus between the Mg-matrix and nanoparticles tends to augment dislocations in nanocomposites. The Orowan bowing mechanism shows how nanoparticles limit the mobility of dislocations in a matrix [37]. The Hall-Petch hypothesis relates the enhanced strength of nanocomposites to grain refining [38]. Squeeze casting was utilized to enhance the grain structure of these nanocomposites and reduce their porosity. Comparing nanocomposites (1% SiC and 1.5%) with the base alloy, the UTS value increased by 42%. This is since the primary and secondary reinforcements are equally distributed throughout the matrix. The hybrid reinforced nanocomposites had the lowest ductility. It is attributed to the inclusion of strong ceramic reinforcements in the Mg matrix. The calculated tensile strength values of this work were found to be similar to the tensile strength values of magnesium-based hybrid nanocomposites developed by Junxiang Zhou et al. [32].

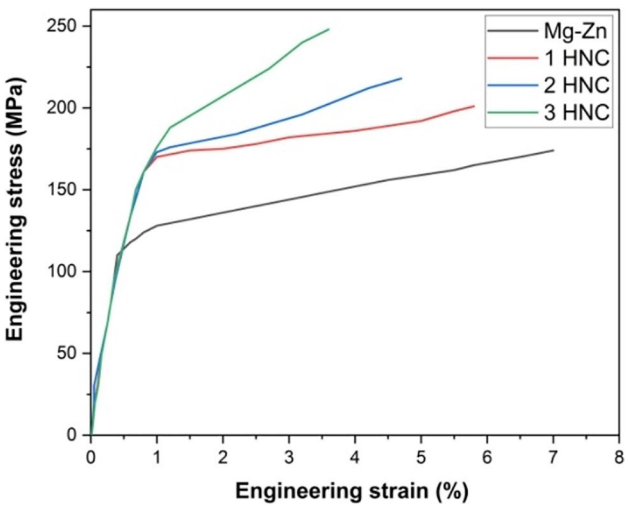

Fig. 4 Stress-strain curves of monolithic alloy and MMNCs

3.2 Hardness Test

The specimen microhardness was determined using a Vickers microhardness tester with OM. The entire experiment was being conducted at room temperature. A 100 g load is applied for 30 s at five separate sites during the specimen's hardness test, and the average values are utilized to calculate the specimen's final hardness value.

The microhardness of nanocomposites varies as a reinforcement function, as represented in Fig. 6. Vickers microhardness rises almost linearly as the base alloy reinforcement

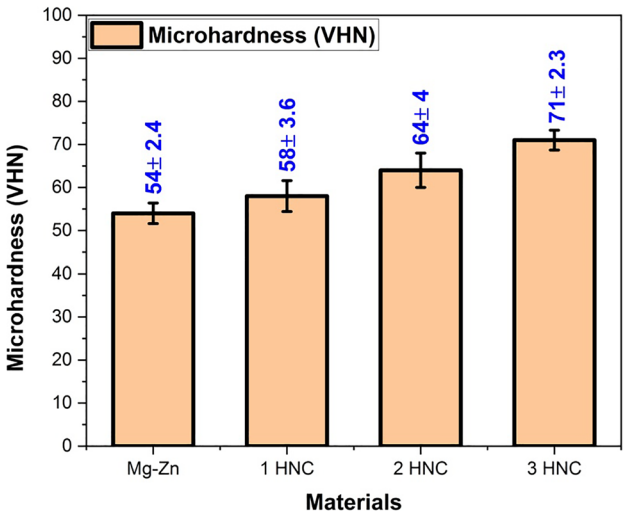

Fig. 6 Microhardness of Mg-Zn alloy and its hybrid nanocomposites

content improves. The nanocomposite has a hard surface than the basic alloy Mg-Zn. It happened due to the inclusion of Silicon Carbide particles, which have a better hardness contrasting the matrix alloy. As the load is applied, these nanoparticles restricted the dislocation motions of an obstacle, resulting in a less penetration depth. The hardness of hybrid reinforced nanocomposites was found to be higher than the base alloy. The microhardness values obtained in this research work was found to be similar to the values reported in the previous literatures [33].

3.3 Microstructure: OPTICAL, SEM, TEM, and XRD

Figure 7 shows optical micrographs of different materials produced by ultrasonic-assisted squeeze casting (Mg-Zn alloy, 1HNC, 2HNC, and 3HNC hybrid nanocomposites). Grain refinement is evident when the SiC concentration in the Mg-Zn alloy matrix is kept constant while the hBN content is increased. Optical micrographs of hybrid nanocomposites and Mg-Zn alloy reveal a substantial difference

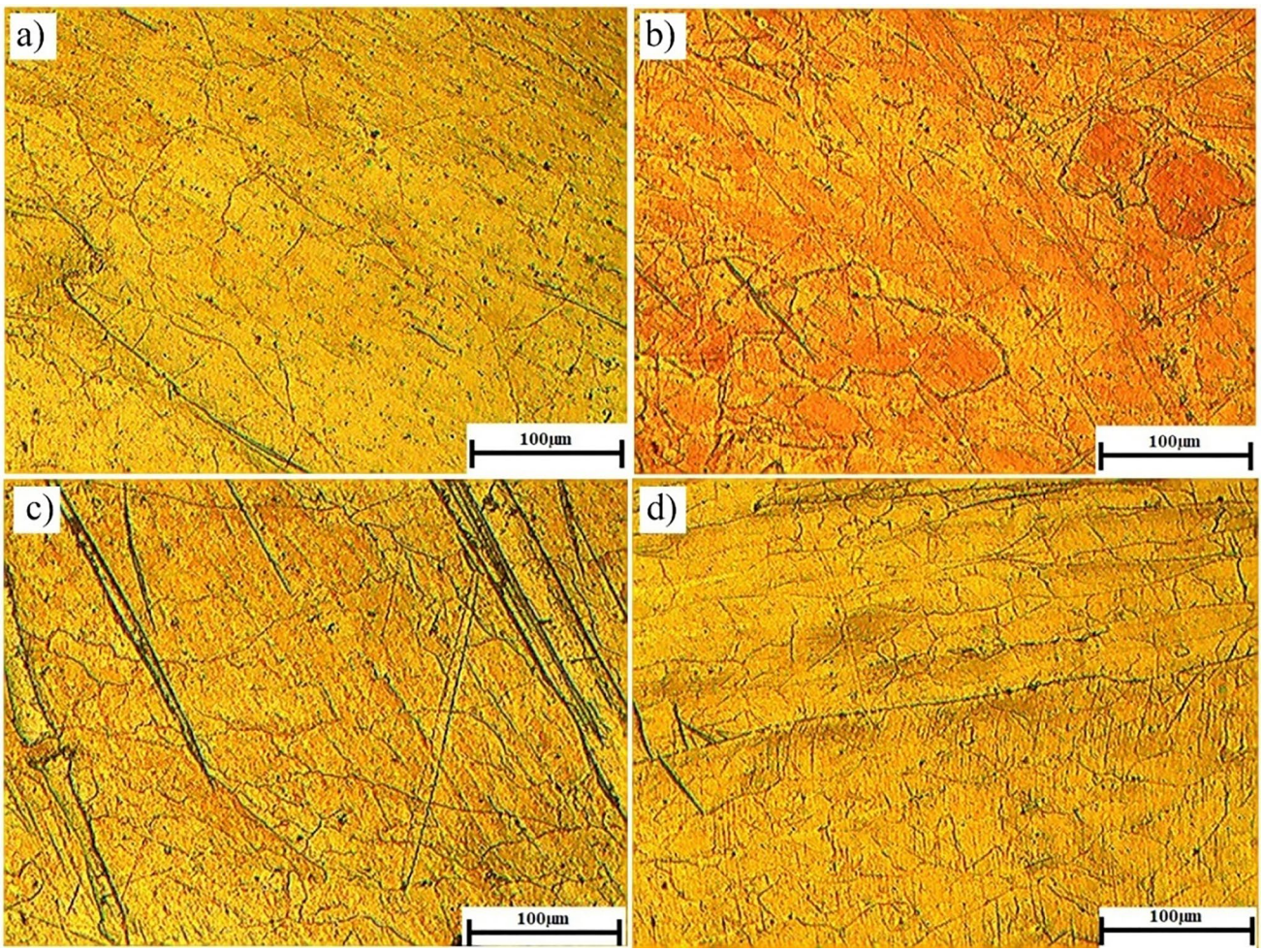

Fig. 7 Optical images of cast samples (**a**) Mg-Zn alloy (**b**) 1HNC (**c**) 2HNC and (**d**) 3HNC

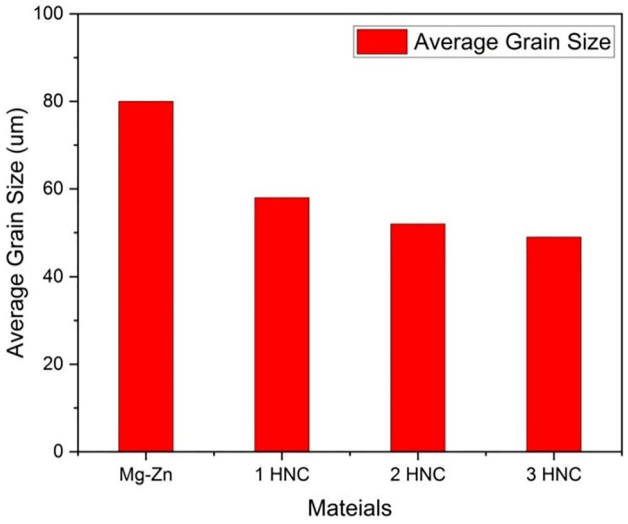

Fig. 8 Variation of mean grain size of Mg-Zn alloy and MMNCs

in grain size. The disparity of mean grain size is shown in Fig. 8. The mean diameter of the grain is 84 µm for Mg-Zn, 58 µm for 1HNC, 52 µm for 2HNC and 49 µm for 3HNC respectively. It is evident from the microstructure of hybrid nanocomposites that the amount of hBN nano reinforcement in the Mg-Zn alloy increases, and the mean size of grain reduce. When comparing to the base alloy, the average grain size reduction is 31%, 38%, and 41% for 1HNC, 2HNC, and 3HNC, respectively. Because of the homogeneous scattering of nanoparticulates in the matrix, quicker nucleation reduces the size of grains as the number of nanoparticles placed in the matrix increases. The reinforcing particles dimension, the nanoparticles weight%, the influence of squeeze casting, and the ultrasonic cavitation impact play a significant role in grain refining.

SEM pictures of Mg-Zn alloy, hybrid nanocomposites 1HNC, 2HNC, and 3HNC are shown in Fig. 9. As shown in Fig. 5b–d, the SiC and hBN reinforcements are evenly distributed across the base matrix. However, as the amount of hBN increases, microstructural clusters of hBN were appeared during SEM investigation.

TEM was performed on a high-resolution JEM 2100 machine for TEM manufactured by JEOL. Wire-cut electrical discharge machining is appropriate for cutting HNC specimens with a thickness of around 3 millimeters (mm). Polishing the wire cut EDM specimens was easy with Emery sheets in grade levels 1200, 1500, and 2000. Using emery

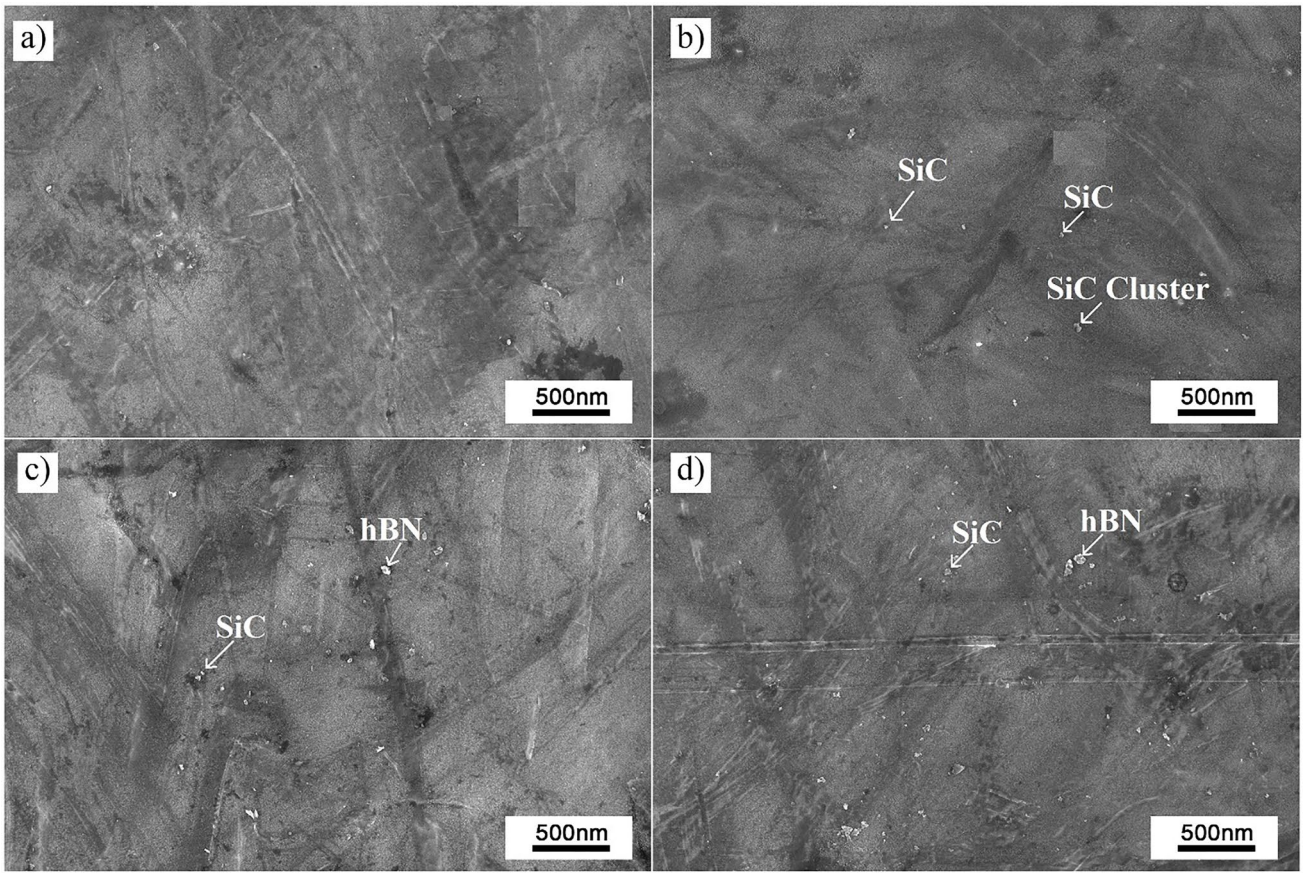

Fig. 9 SEM images particle dispersion (**a**) Mg-Zn alloy (**b**) 1HNC (**c**) 2HNC and (**d**) 3HNC

sheets, each sample is physically polished for more than an hour. The samples are determined to be around 200 nm thick after manual polishing. The samples' thickness is reduced to 50 nm using dimple grinding and ion milling equipment. Punching discs with a diameter of 3mm is done with a disc punch and an ultrasonic disc cutter.

Figure 10 represents the morphology and silicon carbide (SiC) distribution of nanoparticles of hexagonal boron nitride (hBN) in the Mg-Zn/(SiC+hBN) hybrid nanocomposite. Some SiC and hBN nanomaterials are effectively distributed, whereas others are agglomerated, as seen in Fig. 10(a). The SiC and hBN nanomaterials outside the cluster exhibit a homogeneous dispersion when viewed at a high resolution, as seen in Fig. 10(b). In magnesium melt, ultrasonic vibration efficiently disperses SiC and hBN nanoparticles. In the SiCp/Mg-Zn nanocomposite, the interaction between the SiC nanoparticle and the matrix is illustrated in Fig. 10(c). It is validated that at the surface, there is no interfacial reaction. It denotes a strong bond between the SiC nanoparticles and the Mg-Zn alloy.

Increasing the dislocation density of the Mg-Zn/(SiC+hBN) hybrid nanocomposite also increases the strength of the nanocomposite, as represented in Fig. 11(a) and (b).

Figure 12 illustrates the XRD reports of Mg-Zn alloy, 1HNC, 2HNC, and 3HNC hybrid nanocomposites. The kind

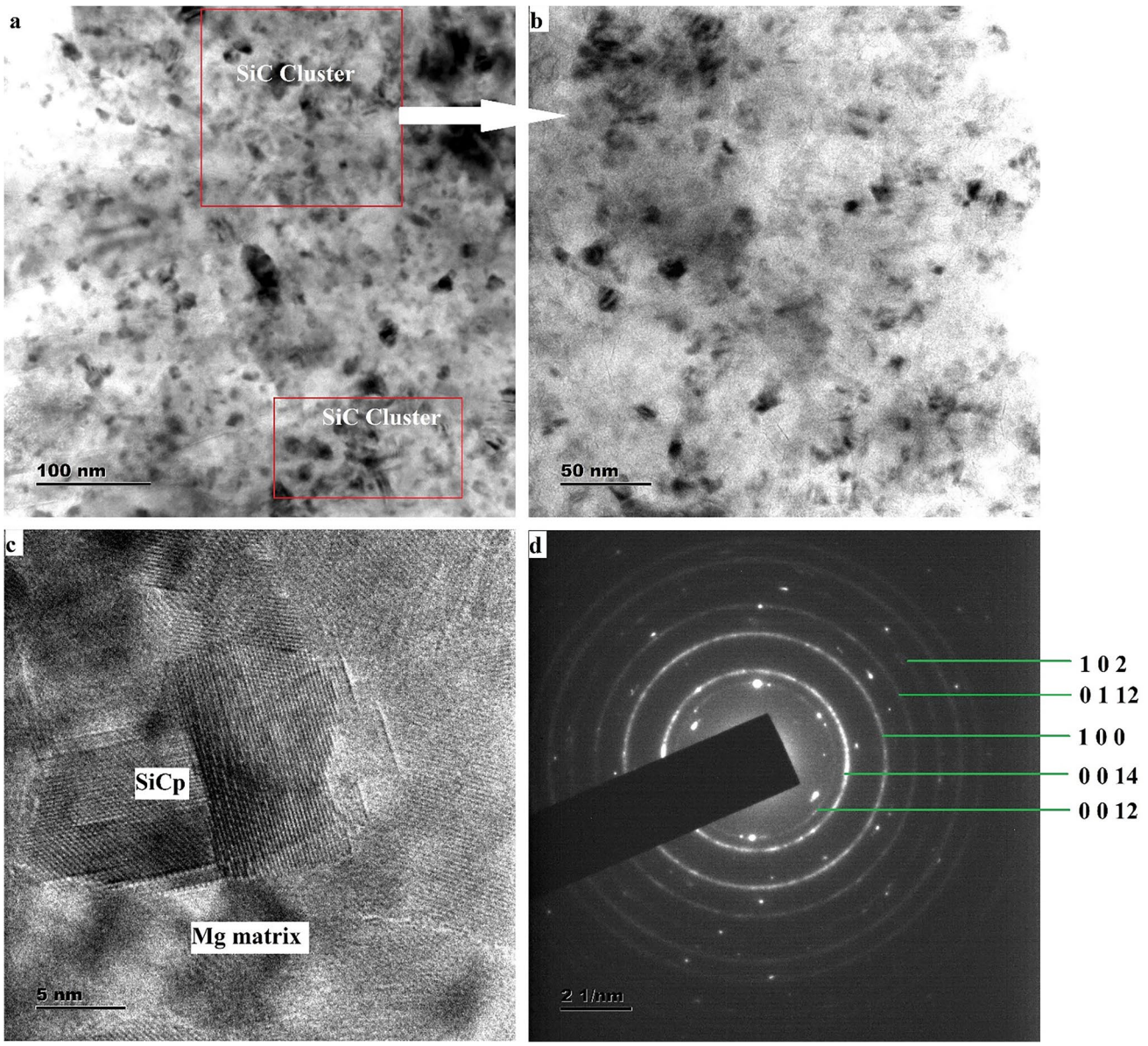

Fig. 10 TEM micrographs of Mg-Zn/(SiC+hBN) (**a**) SiC and hBN dispersion (low magnification) (**b**) SiC and hBN dispersion (high magnification) (**c**) SiC and Mg-Zn interface (**d**) Electron diffraction of SiC and hBN nanoparticles

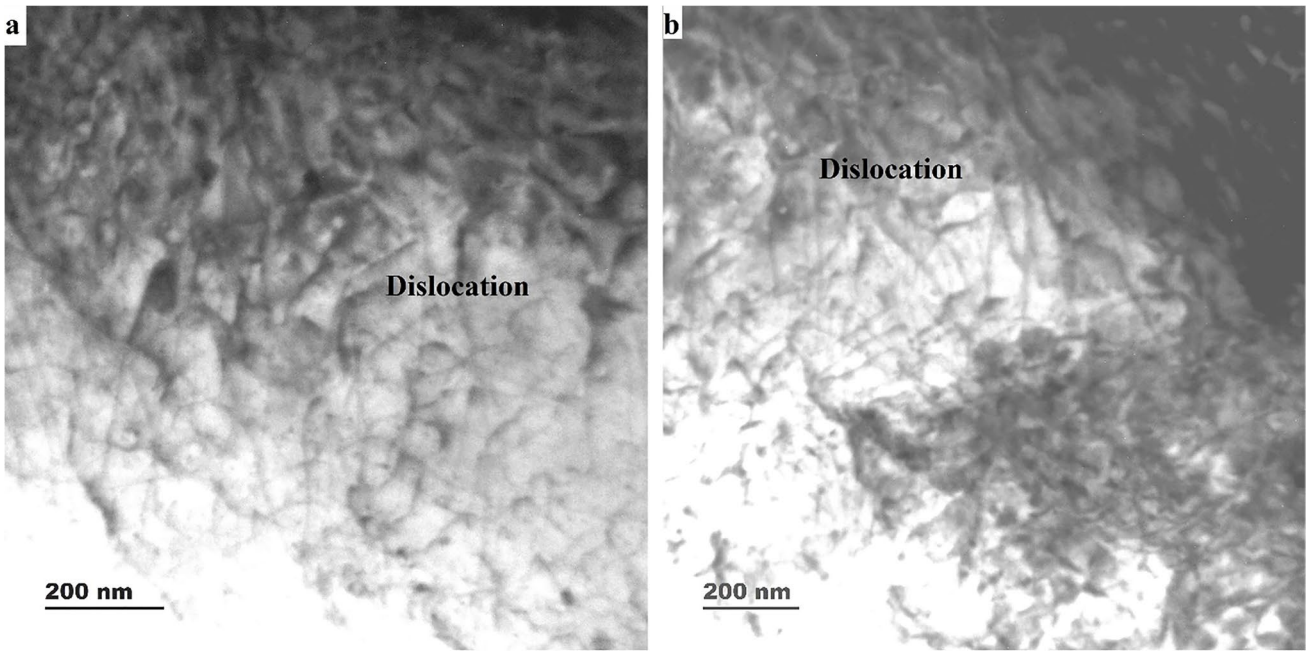

Fig. 11 Typical dislocation arrangements of Mg-Zn/ (SiC+hBN) nanocomposite (**a**) dislocation density of 1HNC hybrid nanocomposite and (**b**) dislocation density of 3HNC hybrid nanocomposite

of reinforcing component has an impact on the properties of hybrid nanocomposites. Different phases of hybrid nanocomposites in XRD investigation were identified by JCPDs software. The intensity peaks of hBN and SiC are lower due to their reduced intensity in the matrix.

4 Grain Refinement Studies – Effect of Sonication/squeeze Casting on Grain Refinement

On solidification, UST may also be employed to improve the microstructure of metallic alloys. The influence of ultrasonic cavitation refining at the course of solidifying has been described with two theories [35]. The initial hypothesis is that ultrasonic boosted the melt's nucleation potential. When ultrasonic cavitation is employed, the heat and pressure characteristics of the melting have changed at high frequencies, which greatly enhanced the nuclei count. Furthermore, ultrasonic cavitation boosts the solute diffusion and augments the nuclei values in the melt by creating intense convection. The second theory proposes that ultrasonic cavitation might create shock waves, causing dendritic tips to break and contributing to microstructure refinement [39–41].

5 Strengthening Mechanisms

Many factors influence the mechanical characteristics of hybrid nanocomposites including manufacturing techniques, matrix strength and grain size, CTE/elastic modulus mismatch, and reinforcement size and wt%. Hall–Petch effect, increased dislocation density, Orowan bowing, and load transfer are some of the predominant strengthening mechanisms in hybrid nanocomposites.

5.1 Hall–Petch Effect

The size of the matrix grain is getting refined by incorporating the nano reinforcements of SiC and hBN in Mg matrix. Refining the grain size would improve the elastic limit of composites. Hall–Petch established a link among the matrix YS and grain diameter. Reducing the grain diameter of the matrix boosts the YS of the MMNCs, as per the Hall–Petch relationship depicted Eq. 1. [36].

$$\Delta\sigma_{HP} = k\left[\frac{1}{\sqrt{d_c}} - \frac{1}{\sqrt{d_m}}\right] \quad (1)$$

Where d_c- mean grain size of SiC and hBN, d_m- average grain size of matrix and k is equal to 0.1 $MNm^{-3/2}$.

5.2 Orowan Strengthening

In practice, it is not suitable to apply the Orowan strengthening mechanism to the MMCs having a reinforcement diameter above5 μm. In nanocomposites, particle size and spacing between the nanoparticles are small, hence dislocation movements are prevented. SiC and hBN nanoparticles function as dislocation barriers, enhancing hybrid nanocomposite yield strength. Equations 2-4 describe the influence

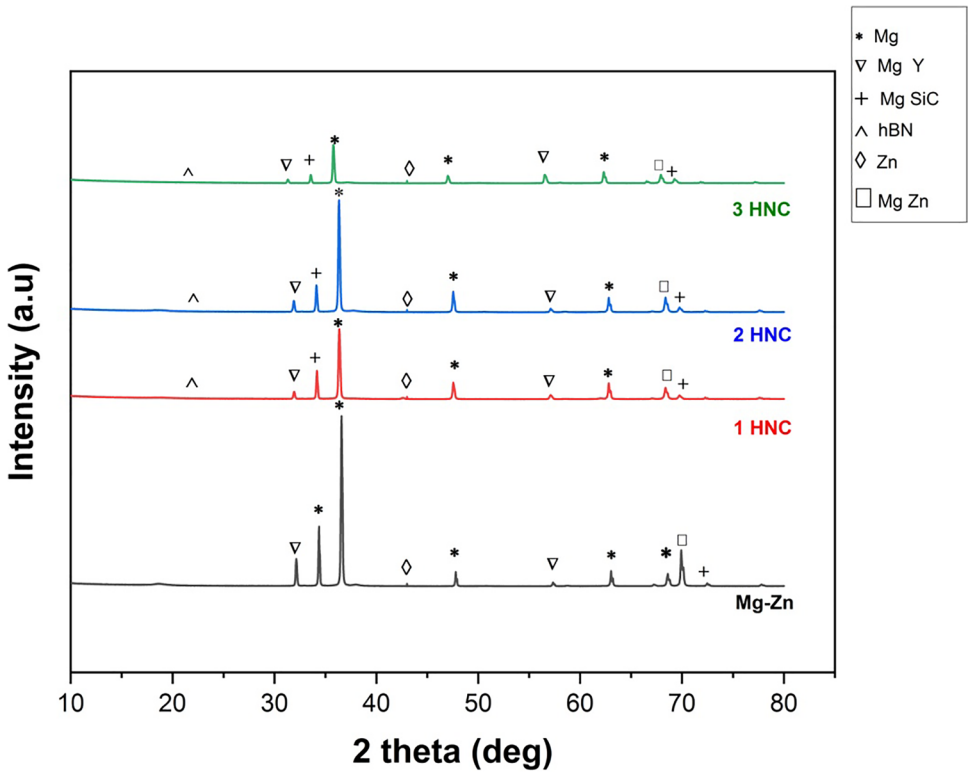

Fig. 12 XRD of Mg-Zn alloy and MMNCs

of Orowan strengthening caused by the SiC and hBN nanoparticle mixture in MMNCs [37].

$$\Delta\sigma_{Orowan} = 0.13 G_m b_m \left[\frac{\ln\left(\frac{d_{SiC}}{2b_m}\right)}{\tau_{SiC}} + \frac{\ln\left(\frac{d_{hBN}}{2b_m}\right)}{\tau_{hBN}} \right] \quad (2)$$

$$\tau_{SiC} = d_{SiC}\left(\left(\frac{1}{2V_{SiC}}\right)^{\frac{1}{3}} - 1 \right) \quad (3)$$

$$\tau_{hBN} = d_{hBN}\left(\left(\frac{1}{2V_{hBN}}\right)^{\frac{1}{3}} - 1 \right) \quad (4)$$

Where $\Delta\sigma_{Orowan}$ is the yield strength variation because of the Orowan effect, G_m is the modulus of shear of the alloy. b_m represents the magnitude of the material Burgers vector. d_{SiC} represents the SiC mean diameter, The mean diameter of the hBN nano reinforcement is denoted by d_{hBN}. The mean inter atomic spacing of SiC is τ_{SiC}. The normal inter particulate spacing of hBN is τ_{hBN}. The volume percentage of SiC nano reinforcements is denoted by V_{SiC}. The volumetric fraction of hBN nano reinforcements is denoted by V_{hBN}. G_m and b_m are 17.3 GPa and 0.32 nm for matrix alloy. SiC nano reinforcement has an average diameter of 50 nm, while hBN nano reinforcement has a standard diameter of 60 nm.

5.3 Dislocation Density

The higher dislocation density in the MMNC as compared with monolithic alloy is attributed to the CTE and elastic modulus mismatch amongst the Mg-Zn and the SiC/hBN nanoparticles. It is possible during the process of cooling during the solidification process. Thus, the empirical relationship provided in Eqs. 5 and 6 are used to determine the increase in thermal stress caused by the geometrically mismatched dislocations [37]:

$$\Delta\sigma_{CTE} = \beta G_m b_m \left(\rho^{CTE}\right)^{\frac{1}{2}} \quad (5)$$

$$\rho^{CTE} = \frac{12\Delta T}{b_m}\left[\frac{\left(\alpha_m - \alpha_{SiC}\right)V_{SiC}}{d_{SiC}\left(1 - V_{SiC}\right)} + \frac{\left(\alpha_m - \alpha_{hBN}\right)V_{hBN}}{d_{hBN}\left(1 - V_{hBN}\right)} \right] \quad (6)$$

Where $\Delta\sigma_{CTE}$ is the variation in elastic modulus because of thermal mismatch, β (constant) is equal to 1.25, G_m represents the matrix rigidity modulus, and b_m is the burger vector magnitude ρ^{CTE} is dislocation density, The SiC mean diameter is denoted by d_{SiC}, The diameter of the hBN is d_{hBN}, α_m denotes the matrix material's thermal expansion coefficients, α_{SiC} is the SiC reinforcement thermal expansion coefficients, α_{hBN} is the hBN reinforcement thermal expansion coefficients, V_{SiC} stands for volume concentration of SiC nano-reinforcements. V_{hBN} stands for the volume fraction of hBN nano-reinforcements. ΔT represents the temperature

variation between the stress-free homologous and room temperatures. ($\Delta T = T_{sf} - T_{room} = 300\ °C - 25\ °C = 275\ °C$).

5.4 Load-bearing Effect

As the ultrasonic cavitation is employed at high frequencies, the formation of variations in the characteristics of the pressure and temperature at the melt helps in potential increase in the number of local nuclei. The relationship given in Eq. 7 describes the load-bearing capacity of nano reinforcement particles [36].

$$\Delta\sigma_{load} = 0.5\left(V_{SiC} + V_{hBN}\right)\sigma_m \tag{7}$$

Where $\Delta\sigma_{load}$ denote a variation in yield strength because of the load-bearing action. V_{SiC} and V_{hBN} represent the volume fraction of SiC_P and hBN_P respectively. σ_m represents the Mg-Zn alloy's yield strength. Table 3 represents the various parameter values which are used to estimate the yield strength of the fabricated MMNCs in this work. The values in the Table 3 were obtained from the previous literatures and the experimental work carried out in the current research. Table 4 indicates the percentage of strengthening contribution of different strengthening mechanisms in 1HNC, 2HNC and 3HNC.

6 Yield Strength Prediction Models

The arithmetic model [38], quadratic summation model [47], compounding models [37], and modified Clyne model [37] are some of the many prediction models useful for analyzing how nanocomposites increase their yield strength.

The phrase "arithmetic summation model" refers to the total of each strengthening mechanism's contributions. The different strengthening effects would work separately and contribute to the hybrid nanocomposites yield strength, according to the Eq. 8 [38].

$$\sigma_{ync} = \sigma_m + \Delta\sigma_{HP} + \Delta\sigma_{load} + \Delta\sigma_{Orowan} + \Delta\sigma_{CTE} \tag{8}$$

For particle reinforced composites with micron size, a quadratic summation model is proposed. Numerous studies indicate that characteristics of the nanocomposite increase. In addition, nanocomposites do not follow the same assumptions as composites reinforced with micron-sized particles. Based on a square root model (Eq. 9), the total improvement in yield strength depends on the sum of all strengthening effects.

$$\sigma_{ync} = \sigma_m + \sqrt{\Delta\sigma_{HP}^2 + \Delta\sigma_{Orowan}^2 + \Delta\sigma_{load}^2 + \Delta\sigma_{CTE}^2} \tag{9}$$

According to the compounding model, as shown in Eq. (10) the increase in yield strength because of nano reinforcements is multiplied by σ_m.

$$\sigma_{ync} = (\sigma_m)\left(1 + \frac{\Delta\sigma_{load}}{\sigma_m}\right)\left(1 + \frac{\Delta\sigma_{CTE}}{\sigma_m}\right)\left(1 + \frac{\Delta\sigma_{Orowan}}{\sigma_m}\right)\left(1 + \frac{\Delta\sigma_{HP}}{\sigma_m}\right) \tag{10}$$

The Orowan and thermal mismatch effects are the primary factors for increasing the hybrid nanocomposite yield strength. While comparing other strengthening mechanisms, the load bearing, and Hall–Petch effects are negligible. The thermal mismatch strengthening mechanisms and Orowan theory have a direct impact on the hybrid nanocomposite's yield strength. Because of this, the square root must be used to add up both Orowan and the thermal mismatch impact. The modified Clyne model indicated in Eq. 11 considers these two strengthening mechanisms when it is squared [37]. Theoretical yield strength values calculated by four different strengthening models and the corresponding experimental

Table 3 Parameters are used in the estimate of yield strength of MMNCs

Parameter	Description	Value	Comment/ Reference
α_m	CTE of matrix	$28.4\times10^{-6}\ °C^{-1}$	[42]
α_{SiC}	CTE of SiC	$4.6\times10^{-6}\ °C^{-1}$	[36]
α_{hBN}	CTE of hBN	$4.563\times10^{-6}\ °C^{-1}$	[43]
K	Constant	$0.1\ MNm^{-3/2}$	[44]
d_c	Average grain size hybrid nanocomposites	58 µm,52 µm, 49 µm	Experimentally obtained value
d_m	average grain size of Mg-Zg alloy matrix	84 µm	Experimentally obtained value
G_m	Rigidity modulus of matrix	16.6 GPa	[45]
b_m	Matrix burgers vector (Magnitude)	0.32 nm	[45]
d_{SiC}	Average diameter of the SiC nanoparticle	50 nm	Average particle size supplied by Manufacturer
d_{hBN}	Average diameter of the hBN nanoparticle	60 nm	Average particle size supplied by Manufacturer
V_{SiC}	Volume fraction of SiC nanoparticle	0.0057	Calculated for 1.0 wt% SiC_P
V_{hBN}	Volume fraction of hBN nanoparticle	0.00435,0.00872,0.0131	Calculated for 0.5 wt%, 1.0 wt% and 1.5 wt% hBN_P
T_{sf}	Stress-free homologous temperature	300 °C	[46]
T_{room}	Room temperature	25 °C	Room temperature
σ_m	Yield strength of matrix	110 MPa	Experimentally obtained value

Table 4 Percentage of strengthening contribution of different strengthening mechanisms in 1HNC, 2HNC and 3HNC

Specimens	Average grain size (μm)	$\Delta\sigma_{HP}$ (MPa)	$\Delta\sigma_{Orowan}$ (MPa)	$\Delta\sigma_{CTE}$ (MPa)	$\Delta\sigma_{load}$ (MPa)
1HNC	58	2.22	31.1	45.06	0.552
2HNC	52	2.95	35.8	53.2	0.793
3HNC	49	3.37	39.54	60.32	1.033

Table 5 Theoretical and experimental YS values

Specimens	σ_{ync} (MPa)				
	Arithmetic summation method	Quadratic summation method	Compounding method	Modified Clyne Model	Experimental value
1HNC	189.13	164.79	204.52	167.52	161
2HNC	202.74	174.19	220.72	177.86	176
3HNC	214.26	182.21	240.98	186.52	188

yield strength values are presented in Table 5. This table explicitly shows that the yield strength values predicted by the modified Clyne and quadratic summation model are very much closer to the experimental yield strength values. Hence, these two strengthening models are highly recommended for predicting the yield strength of the Mg MMNCs.

$$\sigma_{ync} = \sigma_m + \Delta\sigma_{HP} + \Delta\sigma_{load} + \sqrt{\Delta\sigma^2_{Orowan} + \Delta\sigma^2_{CTE}} \quad (11)$$

7 Conclusions

The combined effect of stir-ultrasonication and squeeze casting was successfully applied to produce monolithic Mg-Zn alloy, 1HNC, 2HNC, and 3HNC hybrid nanocomposites. The samples were heat-treated according to T5 heat treatment conditions. Experiments, testing, and characterization lead to the following results.

i. Optical micrographs represent notable grain structure refinement due to the collective effect of sonication and squeeze casting. The grain sizes measured were 84, 58, 52, and 49 μm correspondingly for monolithic Mg-Zn, 1HNC, 2HNC, and 3HNC hybrid nanocomposites.
ii. Ultrasonic streaming and transient cavitation help to disperse the SiC and hBN nanoparticles in Mg matrix. The squeezing effect assists in the reduction of porosity. SEM pictures validated the uniform dispersion of nanoparticles.
iii. Dislocation density in MMNCs is higher compared with the monolith Mg-Zn. The same was confirmed by the TEM images.
iv. XRD validates the SiC, BN, and Yttrium (Traceable) phases in the hybrid nanocomposites.
v. The hard particle dispersion in the nanocomposites significantly inhibits dislocation movements, which increases the yield strength by a considerable amount and marginally lowers the ductility.
vi. Microhardness is increased by 7%, 19%, and 31%, respectively, while comparing 1HNC, 2HNC, and 3HNC MMNCs with the base alloy. The augmentation in microhardness is attributed to the integrated effect of reduction in grain size, Orowan bowing and higher dislocation density.
vii. The yield strength of 1HNC hybrid nanocomposites rises by 46%, that of 2HNC by 60%, and that of 3HNC by 71% when compared with monolithic Mg-Zn. The strengthening contribution of each strengthening mechanism in the decreasing order is denoted as $\Delta\sigma_{CTE}$ - $\Delta\sigma_{Orowan}$ - $\Delta\sigma_{HP}$ -$\Delta\sigma_{load}$.
viii. Yield strength values predicted by the modified Clyne and quadratic summation model are very much closer to the experimental yield strength values.

Acknowledgements (i) The authors acknowledge the financial and facility support (Grant number: CRG/2018/001006) provided by Science and Engineering Research Board (SERB), Govt. of India.

(ii) The authors acknowledge the facility support (Grant number: EEQ/2017/000382) by Science and Engineering Research Board (SERB), Govt. of India.

Author Contributions Parthiban K – Materials procurement, Experimental works, Manuscript preparations, Testing and Characterizations.

Poovazhagan Lakshmanan – Supervising the work, Manuscript corrections, Similarity checking and Corrections.

Gnanavelbabu A – Provided facilities for experimentations, Experimental work – Supervising.

Data Availability This work is part of the ongoing research work. All the data required for this work is included in the manuscript itself.

Declarations

Conflict of Interest The authors declare that they have no known competing financial interests or personal relationships that could have appeared to influence the work reported in this paper.

Consent to Participate Not applicable.

Consent for Publication Not applicable.

References

1. Gupta M, Wong WLE (2015) Magnesium-based nanocomposites: Lightweight materials of the future. Mater Charact 105:30–46. https://doi.org/10.1016/j.matchar.2015.04.015
2. Fan Y, Wu G, Gao H et al (2006) Influence of lanthanum on the microstructure, mechanical property and corrosion resistance of magnesium alloy. J Mater Sci 41:5409–5416. https://doi.org/10.1007/s10853-006-0256-8
3. Shen MJ, Wang XJ, Ying T et al (2016) Characteristics and mechanical properties of magnesium matrix composites reinforced with micron/submicron/nano SiC particles. J Alloys Compd 686:831–840. https://doi.org/10.1016/j.jallcom.2016.06.232
4. Anandajothi M, Vinod B (2020) Tribological behavior of magnesium hybrid composite: effect of amorphous silica-solid waste reinforcement particles to reduce material cost. Silicon. https://doi.org/10.1007/s12633-020-00769-8
5. Kumar KCK, Kumar BR, Rao NM (2021) Microstructural, mechanical characterization, and fractography of AZ31/SiC reinforced composites by stir casting method. Silicon. https://doi.org/10.1007/s12633-021-01180-7
6. Ramesh S, Anne G, Kumar G et al (2021) Influence of ball burnishing process on equal channel angular pressed Mg-Zn-Si alloy on the evolution of microstructure and corrosion properties. Silicon 13:1549–1560. https://doi.org/10.1007/s12633-020-00541-y
7. Rajan K, Bontha R, M R R S et al (2018) Effect of zinc and rare-earth element addition on mechanical, corrosion, and biological properties of magnesium. J Mater Res 33:1–13. https://doi.org/10.1557/jmr.2018.311
8. Huang Y, Xu Y, You S et al (2018) Strengthening and ductilizing of magnesium alloying with heavy rare earth elements. MATEC Web Conf 188
9. Sivashanmugam N, Harikrishna KL (2020) Influence of rare earth elements in magnesium alloy - A mini review. Mater Sci Forum 979:162–166. https://doi.org/10.4028/www.scientific.net/MSF.979.162
10. Gnanavelbabu A, Sunu Surendran KT, Kumar S (2020) Influence of ultrasonication power on grain refinement, mechanical properties and wear behaviour of AZ91D/nano-Al2O3 composites. Mater Res Express 7:16544. https://doi.org/10.1088/2053-1591/ab64d7
11. Agarwal P, Kishore A, Kumar V et al (2019) Fabrication and machinability analysis of squeeze cast Al 7075/h-BN/graphene hybrid nanocomposite. Eng Res Express 1:15004. https://doi.org/10.1088/2631-8695/ab26f5
12. Prasad Reddy A, Vamsi Krishna P, Rao RN (2019) Tribological behaviour of Al6061–2SiC-xGr hybrid metal matrix nanocomposites fabricated through ultrasonically assisted stir casting technique. Silicon 11:2853–2871. https://doi.org/10.1007/s12633-019-0072-9
13. Li J, Lü S, Wu S, Gao Q (2018) Effects of ultrasonic vibration on microstructure and mechanical properties of nano-sized SiC particles reinforced Al-5Cu composites. Ultrason Sonochem 42:814–822. https://doi.org/10.1016/j.ultsonch.2017.12.038
14. Madhukar P, Selvaraj N, Rao CSP, Veeresh Kumar GB (2020) Fabrication and characterization two step stir casting with ultrasonic assisted novel AA7150-hBN nanocomposites. J Alloys Compd 815:152464. https://doi.org/10.1016/j.jallcom.2019.152464
15. Verma P, Kumari P, Ghose J, Pandey V (2019). In: Chattopadhyay J, Singh R, Prakash O (eds) Investigation of mechanical properties and microstructure of pure Al-SiC-nanocomposite casted by stir-squeeze casting process BT - Innovation in materials science and engineering. Springer, Singapore, pp 61–70
16. Wang XJ, Wang NZ, Wang LY et al (2014) Processing, microstructure and mechanical properties of micro-SiC particles reinforced magnesium matrix composites fabricated by stir casting assisted by ultrasonic treatment processing. Mater Des 57:638–645. https://doi.org/10.1016/j.matdes.2014.01.022
17. Madhukar P, Selvaraj N, Gujjala R, Rao CSP (2019) Production of high performance AA7150-1% SiC nanocomposite by novel fabrication process of ultrasonication assisted stir casting. Ultrason Sonochem 58:104665. https://doi.org/10.1016/j.ultsonch.2019.104665
18. Drozd Z, Trojanová Z, Arlic U et al (2017) Effect of hexagonal boron nitride and graphite nanoparticles on the mechanical and physical properties of magnesium. IOP Conf Ser Mater Sci Eng 219:12017. https://doi.org/10.1088/1757-899x/219/1/012017
19. Harichandran R, Selvakumar N (2018) Microstructure and mechanical characterization of (B4C+ h-BN)/Al hybrid nanocomposites processed by ultrasound assisted casting. Int J Mech Sci 144:814–826. https://doi.org/10.1016/j.ijmecsci.2017.08.039
20. Vinod B, Ramanathan S, Ananthi V, Selvakumar N (2019) Fabrication and characterization of organic and in-organic reinforced A356 aluminium matrix hybrid composite by improved double-stir casting. Silicon 11:817–829. https://doi.org/10.1007/s12633-018-9881-5
21. Liu Z, Han Q, Li J (2011) Ultrasound assisted in situ technique for the synthesis of particulate reinforced aluminum matrix composites. Compos Part B Eng 42:2080–2084. https://doi.org/10.1016/j.compositesb.2011.04.004
22. HU K, YUAN D, LÜ S, WU S (2018) Effects of nano-SiCp content on microstructure and mechanical properties of SiCp/A356 composites assisted with ultrasonic treatment. Trans Nonferrous Met Soc China 28:2173–2180. https://doi.org/10.1016/S1003-6326(18)64862-9
23. Soundararajan R, Sivasankaran S, Al-Mufadi FA et al (2019) Investigation on A356-20wt%SiC composites through mechanical stirring and ultra-sonic-assisted cavitation. Mater Res Express 6:96572. https://doi.org/10.1088/2053-1591/ab3082
24. Yuan D, Yang X, Wu S et al (2019) Development of high strength and toughness nano-SiCp/A356 composites with ultrasonic vibration and squeeze casting. J Mater Process Technol 269:1–9. https://doi.org/10.1016/j.jmatprotec.2019.01.021
25. Khandelwal A, Mani K, Srivastava N et al (2017) Mechanical behavior of AZ31/Al2O3 magnesium alloy nanocomposites prepared using ultrasound assisted stir casting. Compos Part B Eng 123:64–73. https://doi.org/10.1016/j.compositesb.2017.05.007
26. Dieringa H, Katsarou L, Buzolin R et al (2017) Ultrasound assisted casting of an AM60 based metal matrix nanocomposite, its properties, and recyclability. Metals 7(10):388

27. Barati F, Latifi M, Moayeri far E, et al (2019) Novel AM60-SiO2 nanocomposite produced via ultrasound-assisted casting; production and characterization. Materials (Basel) 12(23):3976
28. Saboori A, Padovano E, Pavese M, Badini C (2018) Novel magnesium elektron21-AlN nanocomposites produced by ultrasound-assisted casting; microstructure thermal and electrical conductivity. Materials (Basel) 11(1):27
29. Li Q, Qiu F, Dong B et al (2018) Fabrication, microstructure refinement and strengthening mechanisms of nanosized SiCP/Al composites assisted ultrasonic vibration. Mater Sci Eng A 735:310–317. https://doi.org/10.1016/j.msea.2018.08.060
30. Dorri Moghadam A, Omrani E, Lopez H et al (2017) Strengthening in hybrid alumina-titanium diboride aluminum matrix composites synthesized by ultrasonic assisted reactive mechanical mixing. Mater Sci Eng A 702:312–321. https://doi.org/10.1016/j.msea.2017.07.022
31. Lü S, Xiao P, Yuan D et al (2018) Preparation of Al matrix nanocomposites by diluting the composite granules containing nano-SiCp under ultrasonic vibaration. J Mater Sci Technol 34:1609–1617. https://doi.org/10.1016/j.jmst.2018.01.003
32. Zhou J, Ren L, Geng X et al (2019) As-cast magnesium AM60-based hybrid nanocomposite containing alumina fibres and nanoparticles: Microstructure and tensile behavior. Mater Sci Eng A 740–741:305–314. https://doi.org/10.1016/j.msea.2017.10.070
33. Suneesh E, Sivapragash M (2018) Comprehensive studies on processing and characterization of hybrid magnesium composites. Mater Manuf Process 33:1324–1345. https://doi.org/10.1080/10426914.2018.1453155
34. Poovazhagan L, Kalaichelvan K, Sornakumar T (2016) Processing and performance characteristics of aluminum-nano boron carbide metal matrix nanocomposites. Mater Manuf Process 31:1275–1285. https://doi.org/10.1080/10426914.2015.1026354
35. Xuan Y, Nastac L (2018) The role of ultrasonic cavitation in refining the microstructure of aluminum based nanocomposites during the solidification process. Ultrasonics 83:94–102. https://doi.org/10.1016/j.ultras.2017.06.023
36. Nie K, Deng K, Wang X, Wu K (2017) Characterization and strengthening mechanism of SiC nanoparticles reinforced magnesium matrix composite fabricated by ultrasonic vibration assisted squeeze casting. J Mater Res 32:2609–2620. https://doi.org/10.1557/jmr.2017.202
37. Reddy AP, Krishna PV, Rao RN (2019) Strengthening and mechanical properties of SiC and graphite reinforced Al6061 hybrid nanocomposites processed through ultrasonically assisted casting technique. Trans Indian Inst Met 72:2533–2546. https://doi.org/10.1007/s12666-019-01723-y
38. Kim C-S, Sohn I, Nezafati M et al (2013) Prediction models for the yield strength of particle-reinforced unimodal pure magnesium (Mg) metal matrix nanocomposites (MMNCs). J Mater Sci 48:4191–4204. https://doi.org/10.1007/s10853-013-7232-x
39. Xuan Y, Jia S, Nastac L (2017) Processing and microstructure characteristics of As-Cast A356 alloys manufactured via ultrasonic cavitation during solidification. High Temp Mater Process 36:381–387. https://doi.org/10.1515/htmp-2016-0147
40. Jian X, Xu H, Meek T, Han Q (2005) Effect of power ultrasound on solidification of aluminum A356 alloy. Mater Lett 59:190–193. https://doi.org/10.1016/j.matlet.2004.09.027
41. Wang G, Dargusch MS, Qian M et al (2014) The role of ultrasonic treatment in refining the as-cast grain structure during the solidification of an Al–2Cu alloy. J Cryst Growth 408:119–124. https://doi.org/10.1016/j.jcrysgro.2014.09.018
42. Mirza FA, Chen DL (2015) A unified model for the prediction of yield strength in particulate-reinforced metal matrix nanocomposites. Materials 8(8):5138–5153
43. Trojanová Z, Drozd Z, Minárik P et al (2016) Influence of texture on the thermal expansion coefficient of Mg/BN nanocomposite. Thermochim Acta 644:69–75. https://doi.org/10.1016/j.tca.2016.10.010
44. Zhou X, Su D, Wu C, Liu L (2012) Tensile mechanical properties and strengthening mechanism of hybrid carbon nanotube and silicon carbide nanoparticle-reinforced magnesium alloy composites. J Nanomater 2012:851862. https://doi.org/10.1155/2012/851862
45. Lin L, Liu Z, Chen L, Li F (2004) Tensile properties and strengthening mechanisms of Mg–Zn–Zr alloys. Met Mater Int 10:507–512. https://doi.org/10.1007/BF03027411
46. Hassan SF, Tan MJ, Gupta M (2008) High-temperature tensile properties of Mg/Al2O3 nanocomposite. Mater Sci Eng A 486:56–62. https://doi.org/10.1016/j.msea.2007.08.045
47. Srivastava N, Chaudhari GP (2018) Microstructural evolution and mechanical behavior of ultrasonically synthesized Al6061-nano alumina composites. Mater Sci Eng A 724:199–207. https://doi.org/10.1016/j.msea.2018.03.092